Extended Abstracts of the 2004 International Conference on Solid State Devices and Materials, Tokyo, 2004, pp. 940-941

H-10-2

Race-Track Optical Ring Resonators with Groove Coupling

Yuichiro Tanushi, Masaru Wake and Shin Yokoyama

Research Center for Nanodevices and Systems, Hiroshima University
1-4-2 Kagamiyama, Higashi-Hiroshima, 739-8527, Japan
Phone: +81-82-424-6265, Fax: +81-82-422-7185, email: tanushi@sxsys.hiroshima-u.ac.jp

1. Introduction

Recently, optical ring resonator is attracting much attention because of its compactness and applicability to the wavelength division multiplexing and photonic router [1]. Chu *et al.* reported the stack ring resonator, in which the ring and the waveguides are stacked with the spacer, and the coupling efficiency is precisely controlled by the thickness of the spacer [2]. However, the fabrication process is complicated compared with the planer resonators.

In this paper, we have proposed a planer race-track resonator coupled with a groove. The ring and the waveguides are in the same plane and coupled with grooves, in which there remains some thickness of the core film at the bottom of the groove. The groove depth is automatically determined by the loading effect of the plasma etching. Also the race-track resonator enables the precise control of the coupling efficiency by controlling the coupling length even when the groove width is wide.

2. Design of Ring Resonator

We have designed and fabricated the race-track resonators as shown in Figs. 1(a) and 1(b). In the normal planer circle ring resonator with a gap, the gap width is usually less than 0.5 μm and the control accuracy should be less than 0.1 μm [3]. While for the race-track resonator [4], the gap width can be wider because the coupling length L can be lengthened. We have fabricated two kinds of race-track resonators with long coupling length (Fig. 1(a)) and short coupling length (Fig. 1(b)) coupled with grooves. The total length of the rings for (a) and (b) are maintained constant. Firstly we have simulated the light propagation loss of the waveguide with the structure shown in the inset of Fig. 2 for different width. Finite difference method is used in the simulator (Apollo Photonic Solutions Suite). As a result we chose a width of 3 μm because the loss is sufficiently low at the wavelength region around 1.3 μm. Next, the dependence of the bending loss on the curvature radius is simulated (Fig. 3). The radius R=10 μm is used to make compact resonators even the loss is relatively high.

3. Fabrication of Ring Resonator and Measurement

The fabrication procedure is shown in Fig. 4. After the electron beam lithography, the reactive ion etching in CF_4+N_2 plasma is carried out. Because the etching rate in the narrow resist gap is small, the groove is automatically formed between the ring and the coupled waveguides as shown in Fig. 5, while in the other region they are completely separated. Figure 6 shows the schematic sample structure. The sample is cleaved as shown in Fig. 6 and the light output from each waveguide is measured using a semiconductor photodetector and a lock-in amplifier.

4. Results and Discussions

The measured resonating property of the sample shown in Fig. 1(a) is shown in Fig. 7 together with the simulated one. A good agreement between the dip positions in output 1, peak positions in output 2, and simulated resonance positions is obtained. Figure 8 compares the intensities of output 2 for the fabricated two kinds of samples shown in Figs. 1 (a) and 1(b). The output intensity for the sample with longer coupling length is larger. The coupling efficiency for these samples is simulated and plotted in Fig. 9 assuming that the groove reaches to the bottom cladding layer. The difference in the experimental data is smaller than that of the simulated data because some part of the input light propagates through the residual film at the bottom of the groove, while in the simulation the light transfers only through the air gap. Figure 10 shows the resonance characteristics for samples with various groove widths and depths. The groove depth is automatically determined by the groove width due to the loading effect as shown in the table in the figure. It is recognized that the shallower groove leads to the higher output 2 intensity because the coupling is enhanced through the residual film in the groove.

5. Conclusion

We have proposed a new type of race-track resonators coupled with grooves. Good resonance characteristics with high output intensity and good controllability are demonstrated regardless of the simple fabrication process. These results contribute to saving the manufacturing cost of the ring resonators.

Acknowledgement

This study is partially supported by 21st Century COE program "Nanoelectronics for Tera-Bit Information Processing", from the Ministry of Education, Science, Sports, and Culture.

References

[1] B. E. Little *et al.*, J. Lightwave Technol. **15** (1997) 998.
[2] S. T. Chu *et al.*, Photon Technol. Lett. **11** (1998) 691.
[3] B. E. Little *et al.*, Photon Technol. Lett. **10** (1998) 549.
[4] W. Lorattanaruangkit et al., Proc. Asia-Pacific Microwave Conf., 1183 (2000).

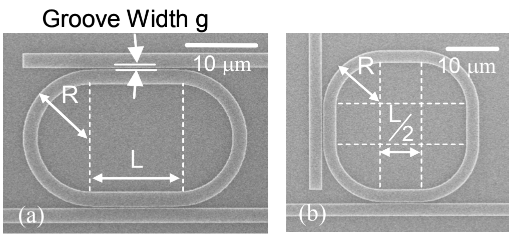

Fig. 1 SEM photographs of the fabricated two kinds of race-track resonators. Coupling length L is (a) 12.6 μm and (b) 6.3 μm respectively. The groove width g is 0.2 μm. Width of the ring and waveguide is 3 μm. Curvature radius R is 10 μm. The total length of the ring is maintained constant at 88 μm.

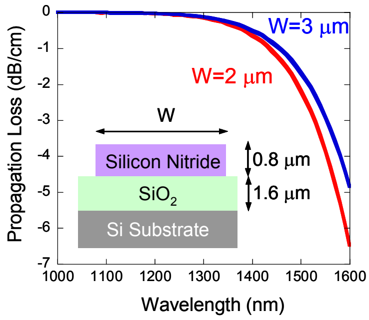

Fig. 2 Simulated propagation loss.

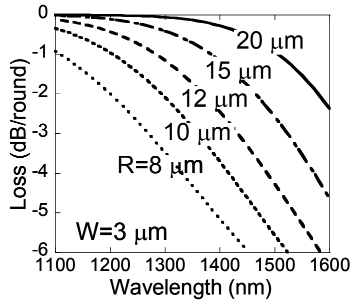

Fig. 3 Simulated bending loss for the circle ring of radius R.

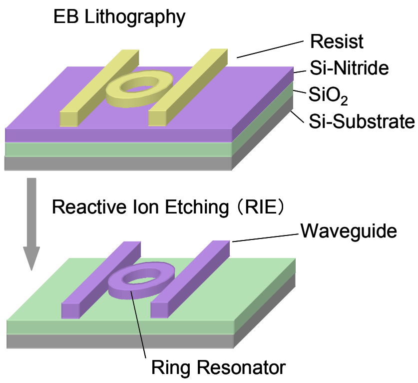

Fig. 4 Fabrication process of the race-track resonator with the coupling groove. Si nitride film is deposited by plasma CVD and SiO_2 cladding layer is thermally oxidized.

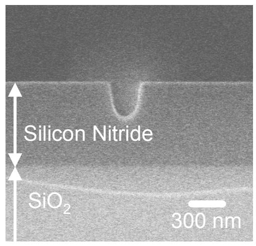

Fig. 5 Cross sectional SEM photograph of the fabricated groove between ring and waveguide. The depth of the groove is automatically determined by the resist gap by the loading effect in the plasma etching.

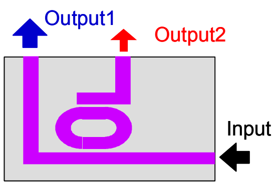

Fig. 6 Schematic figure of the cleaved sample and measurement configuration.

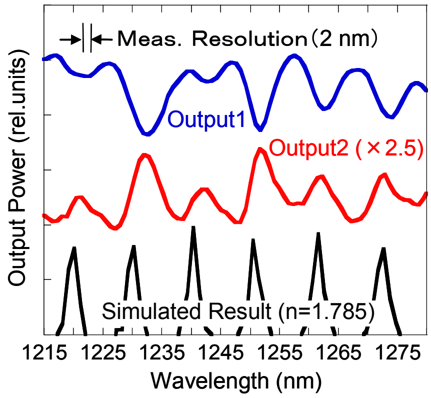

Fig. 7 Measured resonating property of the sample shown in Fig. 1(a). Simulated result is also shown. Simulation method is two dimensional finite difference time domain.

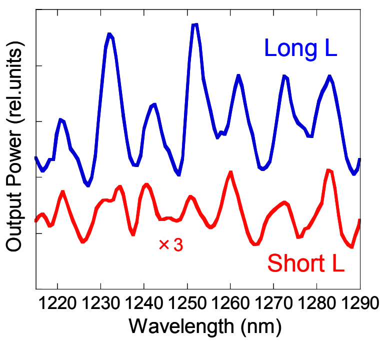

Fig. 8 Comparison between the intensities of output 2 for the fabricated two kinds of samples shown in Figs. 1 (a) and (b).

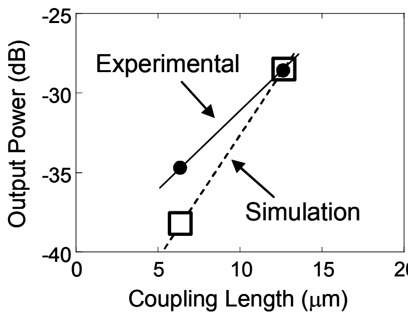

Fig. 9 Power of output 2 for samples (a) and (b) in Fig. 1. For the experimental data for the sample with L=12.6 μm is fit to the simulation because the actual light power is unknown. In the simulation it is assumed that the groove reaches to the bottom cladding layer.

Sample	Groove A	Groove B	Groove C
Width (nm)	100	120	140
Depth (nm)	215	355	555

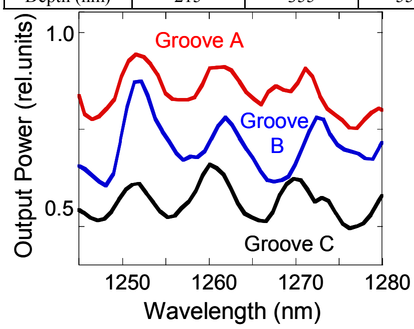

Fig. 10 Resonance characteristics for samples with various groove widths and depths shown in the upper table. The groove depth is automatically determined by the resist gap through the loading effect.